Reprinted from Journal of the Optical Society of America A, Vol. 5, page 1410, September 1988


# Comparison between data and small-angle approximations for the in-water solar radiance distribution

J. Tessendorf

*Areté Associates, P.O. Box 6024, Sherman Oaks, California 91413*

Received October 8, 1987; accepted May 4, 1988

Qualitative and quantitative properties of the in-water distribution of solar radiance, as predicted by the radiative transfer equation, are examined. Two solutions of the radiative transfer equation in the small-angle limit are presented. One of the solutions is the well-known traditional small-angle solution (designated SA). The other (designated SAA) is a solution obtained recently by an approximate evaluation of an exact path-integral expression. In the limit of shallow depth the two solutions are identical, but at depths greater than a certain diffuse path length they differ substantially. Two sets of experimental data are used in comparisons of the apparent solar peak, distribution width, and magnitude as functions of depth. The SAA solution exhibits better qualitative and quantitative agreement with the experimental data than the SA solution. The depth dependence of the diffuse attenuation coefficient obtained from the SAA solution follows that predicted by a finite-difference radiative transfer calculation by Helliwell. At depths greater than approximately six total attenuation lengths, they differ by no more than 5%. The asymptotic diffuse attenuation coefficients predicted by the two approximate solutions are compared with the numerical solution of the corresponding eigenvalue problem. By discretizing the radiative transfer equation, it is shown that the asymptotic diffuse attenuation coefficient is the minimum eigenvalue of a particular matrix, which is constructed explicitly in a simplified two-stream limit. This limiting expression is complementary to the expression obtained from the SAA solution.

## 1. INTRODUCTION

There is a large body of literature on the method of solving the radiative transfer (RT) equation using a small-angle approximation.[1,2] This scheme seems justifiable for many problems in optical oceanography, for example, because the scattering phase function is strongly peaked in the forward direction. When the radiance at the source is confined to a narrow range of directions of propagation—for example, the solar distribution just below the air–sea interface and the emission by a collimated light source—it is reasonable to expect that the distribution will be dominated for many scattering lengths by the region within a few degrees of the peak angle. In such a case many of the properties of the distribution can be calculated from the RT equation near zero degrees (measured from the direction of propagation).

As typically implemented, there are two features of the approximation that reduce the problem to one that can be easily and analytically solved. The first is the restriction to small angles, which removes the dependence of the number of absorption path lengths on the propagation direction. The second is an extension of the angular range from the unit disk to all the two-dimensional plane. The second step permits the use of Fourier transformation of the angular degrees of freedom as well as the spatial ones. The combination of these two steps reduces the RT equation to an inhomogeneous first-order differential equation with constant coefficients, the solution of which is easily obtained.

When compared with experimental data, however, this small-angle solution (which is abbreviated as the SA solution below and outlined briefly in Section 3) fails to predict even qualitatively many properties of the radiance distribution. One suggestion for this disagreement[2] is that the detailed large-angle structure of the phase function has been ignored. This argument implies that the approximation should work best at great depth, because after many scattering lengths the distribution should be dominated in all directions by multiple forward-scattering events. This is not necessarily the case, however. As is shown below, some properties of the distribution predicted by the SA solution agree with the data best at shallow depths.

In addition to ignoring the large-angle structure of the phase function, the SA solution also removes the dependence on propagation direction of the number of absorption path lengths. For light propagating at an angle $\theta$ from the normal to the initial plane of propagation, the intensity is attenuated owing to absorption by the amount

$$\exp(-az/\cos\theta), \tag{1}$$

where $a$ is the absorption coefficient and $z$ is the depth of the plane of observation (parallel to the initial plane). The SA solution approximates $\cos\theta$ by 1 and attenuates the intensity by only

$$\exp(-az).$$

Although the error is small at small angles and shallow depths, the accumulated error at great distances can be substantial. For example, at a depth of ten absorption lengths, the amount of absorption is underestimated by a factor of 2 at an angle of 20°. As will be seen, even at 0° the underestimate can be larger because of the approximation of the scattering contribution.

These two small-angle assumptions—ignoring the large-angle component of the phase function and the directional dependence of the absorption loss—are complementary. Since the phase function for ocean water is broader than the

0740-3232/88/091410-09$02.00 

one used in the SA solution, the amount of scattered radiance at large angles should be larger than predicted. However, absorption of the radiance scattered into large angles should be greater than predicted, reducing the corresponding amount of radiance. The actual distribution combines these competing affects, with the balance depending on the relative strengths of absorption and large-angle scattering.

In the following sections, it is argued that many of the radiant and irradiant properties of the in-water solar distribution can be obtained by using only the small-angle behavior of the phase function and that a more accurate estimate of the absorption loss can be obtained than from the SA solution. The actual balance between scattering and absorption seems to be the following: At shallow depths the absorption path length of the distribution is independent of the propagation direction, as described by the SA solution. At greater depths, however, the dependence of the path length on the propagation direction becomes important, even near the peak of the distribution at 0°. This suppresses the radiance distribution at large angles (more than predicted by the SA solution) and also the importance of large-angle properties of the phase function. The transition from the SA solution to the second behavior is determined by a diffusion length $l$, defined as

$$l^2 = 1/\mu ab, \tag{2}$$

where $a$ and $b$ are the absorption and scattering coefficients, respectively. The mean-squared scattering angle per scattering event, $\mu$, is obtained from the unit normalized phase function $P$:

$$\mu = 2\pi \int_0^\pi \sin^3\theta P(\theta)\mathrm{d}\theta. \tag{3}$$

The small-angle solution presented in Section 3 accounts for this behavior and is designated the SAA solution because it is identical in formulation to the SA solution, with the exception that it includes a dependence on propagation direction in the absorption loss.

The meaning of the diffusion length $l$ and the differences between the SA and SAA solutions can be illustrated as follows: Consider a small volume of radiant energy propagating in some direction. The operational definition of a small volume is that the distribution of energy within the volume can be neglected as it propagates. In this case the volume can be considered pointlike. The point of light traverses the medium following a path that is curved owing to scattering and is diminishing in intensity because of absorption. The path is an accumulation of a random walk in the direction of propagation. Over short distances little scattering occurs, and the absorption loss is insensitive to the narrow angular deflection that the light has suffered. The possible set of paths is determined by the phase function and initial conditions alone, and the random walk in the direction of propagation is essentially diffusive. Over distances longer than the diffusive path length $l$, the set of paths that the light may take includes a substantial number at large angles to the initial direction of propagation, for which the absorption loss is more severe because of the larger path length. The light reaches great depths by avoiding large-angle scattering events, and as a result the large-angle properties of the phase function are effectively suppressed. In this situation the random walk in the propagation direction is bounded in its directional character and is nondiffusive. The length scale $l$ characterizes the transition from a diffusive to a nondiffusive random walk.

This interpretation in terms of a random walk of a point of light suggests that RT may be formulated in terms of statistical quantities. Indeed, the RT equation can be obtained from the theory of wave propagation in random media,[3] and one of the methods of numerical solution is the Monte Carlo technique.[4] Thebaud and Gayer[5] used a random-walk analysis in the small-angle approximation to solve the problem of transfer in a stratified medium. An exact solution of the RT equation in terms of path integration exists[6] and corresponds to a sum over all possible paths of the attenuated contribution of each path. This solution is reviewed in Section 2, and from it both the SA and the SAA approximate solutions are constructed in Section 3. Although the SA solution can be obtained by simpler methods, it is instructive to see the diffusive nature of the SA solution come from the path-integral approach.

To see the effect of including some dependence on direction in the absorption, the SA and the SAA solutions are compared in Section 4 with each other and with published experimental data[7,8] on the in-water distribution of solar radiance. The quantities compared are the angular width and peak location of the distribution as functions of depth and the actual distribution at several orientations and depths. Whereas the SA solution generally does a poor job of reproducing these quantities, the SAA solution enjoys at least a qualitative agreement with the data.

In addition to comparisons with experimental data, the asymptotic diffuse attenuation coefficient $K_d$ predicted by the two solutions is compared in Section 5 with the result of Prieur and Morel[9] for the numerical solution of the corresponding eigenvalue problem. By discretizing the angular degrees of freedom, the RT equation is converted to a matrix of equations that can be exactly solved. From that solution it is shown that $K_d/c(c = a + b)$ is the minimum eigenvalue of a particular matrix. As a simple approximate example, a two-stream discretization is used to obtain the eigenvalue. This two-stream calculation of $K_d$ can be made to agree reasonably with the numerical solution when scattering dominates absorption. This is complementary to the SAA expression, which can be made to work reasonably well when absorption dominates scattering.

Also of interest is the depth dependence of the diffuse attenuation coefficient $K_d(z)$, and this is also discussed in Section 5. The SAA and SA solutions are compared with numerical results obtained by Helliwell and Gasster.[10,11] The SAA solution for $K_d(z)$ is an improvement over the SA solution only for depths approaching the asymptotic limit at about six total attenuation lengths.

Section 6 contains some conclusions and discussion on the nature of the small-angle approximation as the leading-order expression of an expansion scheme.

An ultimate goal of this type of study of the RT equation is to develop an ability to predict accurately and quantitatively details of the in-water radiance distribution, using as little numerical computation as possible to extend the practical applicability of the predictions. The scope of this paper is less ambitious, however, concentrating on the issue of the

degree of improvement obtained when a more nearly complete approximation is made within the small-angle assumption. When the SA and SAA forms of the small-angle approximation are compared with experimental and numerical data, the basic result obtained is that the small-angle approach can provide more-accurate information than just the SA solution. The improvement is still inadequate in many regards, however; e.g., it is incapable of predicting properties of the upwelling light field. Nevertheless, this result could be useful in several aspects of ocean optics: for the theorist developing numerical or analytical schemes it can provide a benchmark to indicate the extent to which additional sophistication provides additional gains, and for the empiricist it can suggest parametric forms for quantities of interest that can be fitted to experimental data to determine the parameters.

Before we discuss the solution of the RT equation in Section 2, the quantities of interest are defined in this paragraph. The radiance $L$ at depth $z$ satisfies the equation

$$\left[\eta(n)\frac{\partial}{\partial z}+\mathbf{n}\cdot\nabla+c\right]L(\mathbf{x},\mathbf{n},z)=b\int \mathrm{d}^2n'P(\mathbf{n},\mathbf{n}')L(\mathbf{x},\mathbf{n},z), \tag{4}$$

with the initial condition

$$L(\mathbf{x},\mathbf{n},z=0)=L_0(\mathbf{x},\mathbf{n}).$$

In these equations $\mathbf{x}$ is the position in any plane normal to the $z$ axis. The vectors $\mathbf{n}'$ and $\mathbf{n}$ are the components normal to the $z$ axis of the direction unit vector:

$$\mathbf{n}=\hat{n}-(\hat{n}\cdot\hat{z})\hat{z},$$

and

$$\eta(n)=\hat{n}\cdot\hat{z}=(1-n^2)^{1/2}$$

is restricted to the forward direction only. The coefficients $c$ and $b$ have been defined.

## 2. SOLUTION BY SUM OVER PATHS

In Ref. 6 an exact solution of the RT equation was constructed for the problem of finding the forward-scattered radiance at any plane $z$ = constant below the initial data plane $z = 0$. The solution is expressed in terms of a path integral over all possible paths that light can take from an initial direction of propagation $\mathbf{n}'$ at $z = 0$ to the direction of propagation $\mathbf{n}$ at depth $z$. Backscatter of light in not included in this solution. The path taken is the accumulation of the propagation direction at each depth. The path-integral solution associates with each path an effective number of attenuation lengths $\tau$ that are due to absorption and scattering, and the radiance is proportional to

$$L\sim\sum_{\text{paths}}\exp[-\tau(\text{path})].$$

If the phase function is forward peaked, the sum is approximately equal to the contribution from the path with the smallest effective attenuation, plus fluctuations about that path. The small-angle solutions given in Section 3 are constructed by approximating the expression for $\tau$. The differences in the solutions arise from different expressions for the paths with the lowest attenuation and also for the extent of fluctuations about those paths.

For a specific path, suppose that $\beta(z')$ is the direction vector at depth $z'$, satisfying the boundary conditions

$$\beta(0)=\mathbf{n}',$$

$$\beta(z)=\mathbf{n}.$$

The number of absorption lengths according to expression (1) is

$$\tau_a=a\int_0^z \mathrm{d}z'\frac{1}{\eta[\beta(z')]}. \tag{5}$$

The attenuation from the accumulation of scattering events is derived in Ref. 6. Assuming that the phase function is peaked in the forward direction and depends only on its rms angular width[6],

$$\tau_b=\frac{1}{2\mu b}\int_0^z \mathrm{d}z'\frac{1}{\eta[\beta(z')]}\left(\frac{\partial\beta(z')}{\partial z'}\right)^2. \tag{6}$$

From these two contributions, the path-integral expression for the solar distribution is

$$L(z,\mathbf{n})=N\int[D\beta]\delta(\beta(0)-\mathbf{n}_s)\delta(\beta(z)-\mathbf{n})\times\exp\{-[\tau_a(\beta)+\tau_b(\beta)]\}, \tag{7}$$

where $[D\beta]$ is the integration measure,

$$[D\beta]=\prod_0^z \mathrm{d}^2\beta(z'),$$

and each $\mathrm{d}^2\beta$ in the measure is over the unit disk. The normalization constant $N$ is determined by the condition

$$L(z=0,\mathbf{n})=I_s\delta(\mathbf{n}-\mathbf{n}_s),$$

where $\mathbf{n}_s$ is the direction vector for the solar radiance at the initial plane and $I_s$ is the downward solar intensity at the surface $z = 0$.

A point of light that follows the direction vector $\beta(z')$ as it propagates is located relative to its initial position at

$$\mathbf{R}(z)=\int_0^z \mathrm{d}z'\beta(z')/\eta[\beta(z')]$$

in the plane at depth $z$. Although the path $(\mathbf{R}, z)$ describes the position of the point of light as it traverses the water, the discussion in the remaining sections is based on the direction vector $\beta$. The two points of view contain the same information, and the term "path" is applied to either.

## 3. SMALL-ANGLE SOLUTIONS

The path-integral expression in Eq. (7) cannot be evaluated analytically. Methods exist to evaluate the integral approximately, however, principally by approximating the integrand by a Gaussian form. Gaussian path integrals can be evaluated.[12] The path that contributes most to the radiance is the path that minimizes the total attenuation $\tau_a + \tau_b$ and is called the stationary path, $\beta_0(z')$. The approximate evaluation of the path integral includes only this stationary path

and surrounding paths that deviate only a small amount from $\beta_0$. The result is

$$L(z, \mathbf{n}) \sim I_s D(\beta_0) \exp\{-[\tau_a(\beta_0) + \tau_b(\beta_0)]\},$$

where $D$ includes the normalization constant $N$ and a determinant contributed by the surrounding paths.

In the SA approximation, the terms that behave as $\cos\theta$ are replaced by 1, so that $\eta(\beta) \to 1$, and the total attenuation is

$$\tau_a + \tau_b = az + \frac{1}{2\mu b}\int_0^z dz' \dot{\beta}^2(z').$$

The stationary path that minimizes this attenuation is

$$\beta_0(z') = \mathbf{n}_s + \frac{z'}{z}(\mathbf{n} - \mathbf{n}_s).$$

Note that the absorption loss is independent of path in the SA approximation and that the stationary path is determined by the scattering attenuation alone. The stationary path uniformily changes from the initial direction of propagation $\mathbf{n}_s$ to the final one $\mathbf{n}$ without suffering increased absorption loss as the path length normal to $\mathbf{n}_s$ increases. As is seen in Section 4, the result is that the solar distribution predicted by this approximation is too broad and is not attenuated sufficiently.

In evaluating the path integral, the determinant in the SA approximation varies with the depth as

$$D \sim z^{-1},$$

and the radiance distribution is

$$L_{\mathrm{SA}}(z, \mathbf{n}) = \frac{I_s}{2\pi\mu b z} \exp\left\{-\left[az + \frac{(\mathbf{n} - \mathbf{n}_s)^2}{2\mu b z}\right]\right\}. \quad (8)$$

This distribution is Gaussian, and its width increases with depth as $z^{1/2}$, which is characterstic of a diffusive random walk.

To construct the SAA solution, terms that behave as $\cos\theta$ are approximated just as in the SA solution. However, the dependence on $\eta(\beta)$ in the absorption term in Eq. (7) is approximated not by 1 but by

$$\frac{a}{\eta(\beta)} \to a\left(1 + \frac{1}{2}\beta^2\right).$$

The total attenuation in this case is

$$\tau_a + \tau_b = az + \frac{1}{2\mu b}\int_0^z dz'[\dot{\beta}^2(z') + \beta^2(z')/l^2],$$

and $l$ is the length scale defined in Eq. (2). In this approximation the total attenuation has a path-dependent contribution from absorption. The stationary path also depends on the absorption through the length scale $l$. In fact,

$$\beta_0(z') = \mathbf{n} f(z') + \mathbf{n}_s f(z - z'),$$

where

$$f(z') = \frac{\sinh(z'/l)}{\sinh(z/l)}.$$

For propagation to depths $z \ll l$, this stationary path is essentially the diffusive one found for the SA solution. For depths comparable with or greater than $l$, however, this stationary path is different. The absorption dependence confines the stationary path to a region around the initial propagation direction that is narrower than in the SA solution (see Fig. 1). The transition to the final direction of propagation $\mathbf{n}$ occurs at a depth $z'$ close to $z$. In this region the rapid change in the propagation direction must be accomplished by scattering events over larger angles than occur in the SA approximation. The resulting distribution is narrower than the SA solution because of this confinement and is lesser in magnitude than the SA solution because of the additional path-dependent absorption loss.

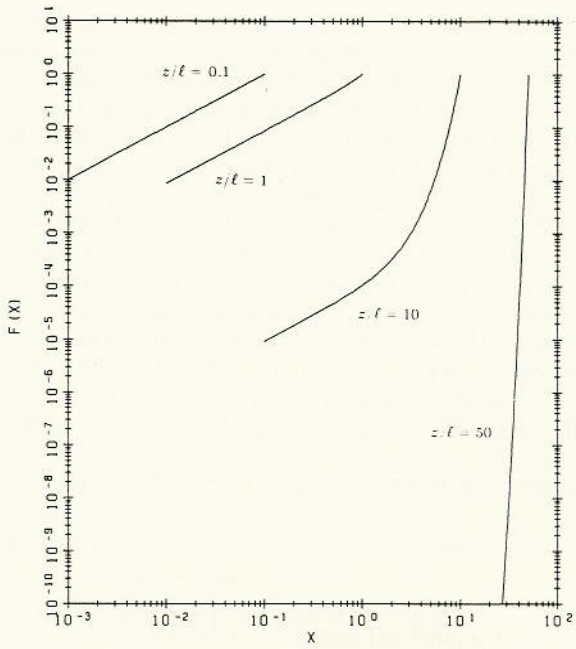


Fig. 1. The function $f(z')$ for several values of $z/l$.

The increased loss in the SAA solution reduces the contribution of the paths surrounding the stationary path. Their contribution varies with depth as

$$D \sim [\sinh(z/l)]^{-1},$$

which is smaller than for the SA solution except in the limit $z \ll l$. The SAA solution for the radiance distribution is[6]

$$L_{\mathrm{SAA}}(z, \mathbf{n}) = \frac{I_s}{2\pi\mu b l \sinh(z/l)} \exp\{-[az + A(z/l, \mathbf{n}, \mathbf{n}_s)]\}, \quad (9)$$

where

$$A(x, \mathbf{n}, \mathbf{n}_s) = [2\mu b l \sinh^2(x)]^{-1} \times \left[\frac{n^2 + n_s^2}{2}\sinh(2x) - 2\mathbf{n}\cdot\mathbf{n}_s \sinh(x)\right]. \quad (10)$$

Note that in the limit $z/l \to 0$, Eq. (9) reduces to Eq. (8).

## 4. COMPARISON WITH EXPERIMENTAL DATA

Although the SA and SAA small-angle solutions originate from similar expressions, the distributions predicted by the two are different. To illustrate this, several properties of

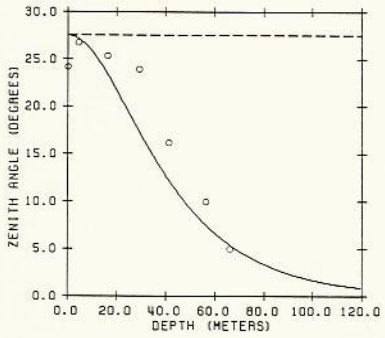


Fig. 2. Peak of the solar distribution according to the SAA (solid curve) and SA (dashed line) approximations, and data.

the solar distribution are calculated from the solutions and compared with one another and with experimental data. The experimental data used are the data obtained by Tyler[7] on the solar radiance distribution in Lake Pend Oreille and the data on the width of the solar distribution obtained by Browne and Axford[8] off the Southern California coast. The quantities compared are the width of the distribution as a function of depth, the peak angle of the distribution as a function of depth, and the relative radiance distribution has a function of depth and orientation. In addition, Section 5 contains a comparison of the asymptotic diffuse attenuation coefficient predicted by the two solutions with two other calculations based on eigenvalue methods.

The optical properties $a$, $b$, and $P$ of the water in the two experiments must be known if the comparisons are to be made. Browne and Axford give only the diffuse attenuation coefficient. As is shown below, however, the SAA solution for the width of the solar distribution behaves in a qualitatively correct way, and the one quantity needed to compare with Browne and Axford's data can be estimated from the data. Preisendorfer[13] published the optical properties for the Lake Pend Oreille data. From that list, the values used are

$$a = 0.12\ \mathrm{m}^{-1},$$

$$b = 0.3\ \mathrm{m}^{-1},$$

$$\mu = 0.035.$$

In addition, the solar zenith was $\theta_{\mathrm{Sun}} = 27.5°$. This gives a diffusion length of $l = 28$ m. Data from Lake Pend Oreille were reported to a depth of 66.1 m, which is 26 extinction lengths.

**Solar Peak**

From Eqs. (8) and (10), the apparent peak angle of the solar distribution predicted by the SA approximation is

$$\theta_p^{\mathrm{SA}} = \theta_s,$$

i.e., the peak of the distribution remains in the direction of the Sun regardless of depth. The SAA prediction is

$$\theta_p^{\mathrm{SAA}} = \arcsin\left[\sin\theta_s \frac{2\sinh(z/l)}{\sinh(2z/l)}\right],$$

which asymptotically approaches 0° with depth. The solid curve in Fig. 2 shows the SAA prediction for Tyler's data. The dashed line is the SA prediction. The plotted data

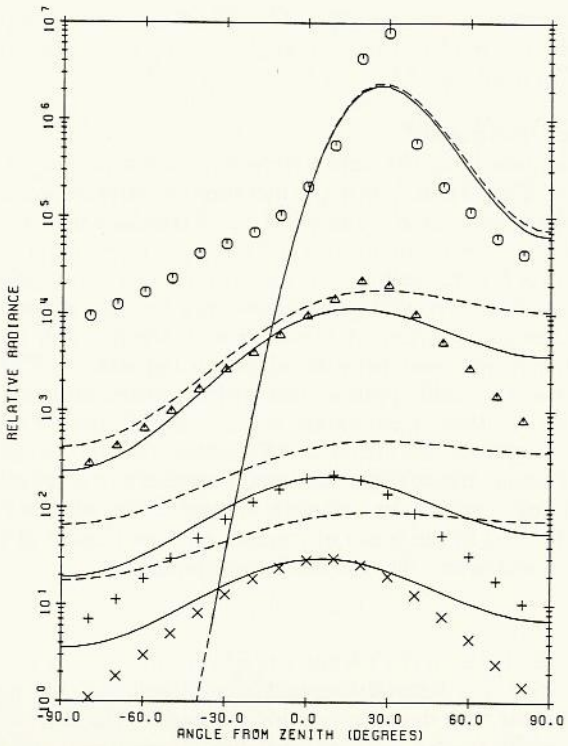


Fig. 3. Radiance distribution in the plane of the Sun and instrument, at depths of 4.24, 29, 53.7, and 66.1 m. The solid and dashed curves are from the SAA and SA approximations, respectively.

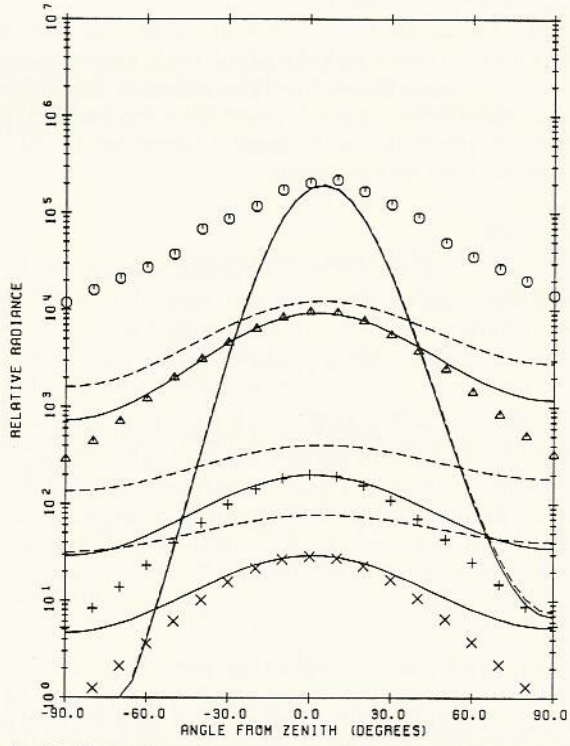


Fig. 4. Radiance distribution 80° from the plane of the Sun and instrument, at depths of 4.24, 29, 53.7, and 66.1 m. The solid and dashed curves are from the SAA and SA approximations, respectively.

points were taken from Ref. 14. The SAA solution reproduces the trend of the peak angle toward zero with depth seen in the data.

### Solar Distribution

Using data from the extensive set of tables published by Tyler,[7] Figs. 3 and 4 show the measured relative radiance at depths of 4.24, 29, 53.7, and 66.1 m. To make comparisons with these distributions, it was necessary to know the solar intensity $I_s$ at the initial surface. Alternatively, the approximate solutions could be normalized at a depth to agree with the data at a particular direction and depth. The latter approach was used because, although the data at 4.24-m depth are probably representative of the distribution at the surface, neither approximate solution is sufficiently accurate to replicate the strong non-Gaussian peak in the distribution near the surface. Since the approximate solutions are more likely to be accurate at depth, the peak in the distribution in the plane of the Sun and instrument at $z$ = 66.1 m was used. The normalization constant

$$I_s = 1{,}040{,}000$$

was used for both the SA and the SAA solutions. As can be seen from the figures, the rate of extinction of the peak magnitude with depth is reproduced well by the SAA solution, while the SA solution does not attenuate so rapidly. The reason for the difference lies in the difference between the approximations: the SA solution does not provide for additional attenuation over paths that are longer in the horizontal direction.

Neither solution predicts the roll-off of the distribution at angles larger than 10°–15° away from the solar peak, although the SAA solution is noticeably narrower than the SA solution. This limitation provides an operational definition of the range of validity of the small-angle approximation. As is demonstrated below, however, although the width of the SAA distribution is much larger than the data, at least the trend in the width as the depth is increased is qualitatively reproduced by this solution.

### Solar Width

The $e^{-1/2}$ widths of the two solutions are

$$\sin^2 \theta_{1/2}{}^{\mathrm{SA}} = \mu b z, \tag{11}$$

$$\sin^2 \theta_{1/2}{}^{\mathrm{SAA}} = 2\mu b l \frac{\sinh^2(z/l)}{\sinh(2z/l)}. \tag{12}$$

Notice that the width predicted by SA grows without bound, whereas the SAA width asymptotically approaches a limit. The second behavior is in qualitative agreement with observations. Browne and Axford[8] reported measurements off the California coast of the full width at half-maximum, which is related to the $e^{-1/2}$ width by

$$\sin^2(\theta_{\mathrm{FWHM}}/2) = (\log_e 4) \sin^2 \theta_{1/2}.$$

Unfortunately, the only optical property that they report is the diffuse attenuation length, which was measured to be essentially constant with depth at $K_d$ = 0.08 m$^{-1}$. From Section 5 below, the diffuse attenuation coefficient $K_d$ is connected to $c$, $b$, and $P$ by the approximate expression

$$K_d = a + 1/l.$$

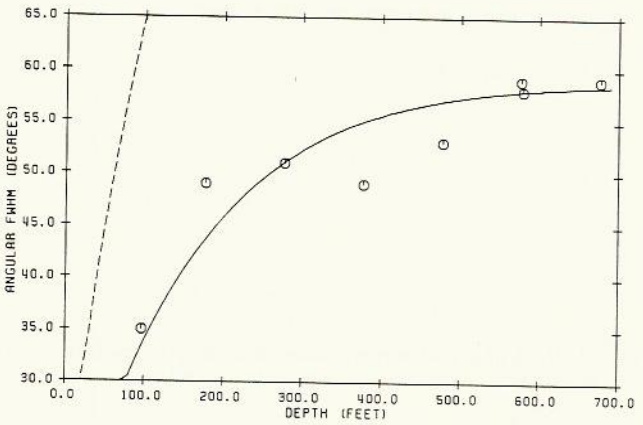


Fig. 5. Full width at half-maximum for the solar distribution. The solid curve is the SAA prediction, and the dashed curve is the SA prediction. The circles are the measurements by Browne and Axford.

The data indicate that the FWHM approaches an asymptotic value of $\theta_{\mathrm{FWHM}} \sim 59°$ at large depth. In fact, the form of Eq. (12) shows that the SAA approximation predicts that the asymptotic value

$$\sin^2(\theta_{\mathrm{FWHM}}{}^{\mathrm{SAA}}/2) \to (\log_e 4)\mu b l$$

is achieved when $z \gg l$. With these two relations, the implied parameters are

$$\mu b l = 0.18,$$

$$l = 83 \text{ m}$$

$$a = 0.069 \text{ m}^{-1},$$

$$\mu b = 0.002 \text{ m}^{-1}.$$

Figure 5 shows the data reported by Browne and Axford (circles). The solid curve is the prediction by the SAA approximation, and the dashed curve is predicted by the SA approximation. As can be seen from Fig. 5 and Eq. (11), the SA width grows without bound, whereas the SAA width is consistent with the experimental data in approaching an asymptotic value.

## 5. DIFFUSE ATTENUATION

Water's optical properties are categorized as either inherent or apparent propeties. The inherent properties $c$, $b$, and $P$ depend only on the characteristics of the water that cause absorption and scattering of light. The apparent properties are the quantities that are more frequently and easily measured, such as the diffuse attenuation coefficient $K_d$. These quantities depend not only on the inherent properties but also on the distribution of light around the measuring device. One of the problems of current interest in optical oceanography is the relationship between inherent and apparent properties. The most rigorous mathematical work in this area has been on the diffuse attenuation coefficient. Preisendorfer[15] showed that as the depth becomes large, $K_d$ approaches a form that is independent of the radiance distribution and depth and depends only on $c$, $b$, and $P$ in the form

$$K_d(\infty) = cg(b/c, P),$$

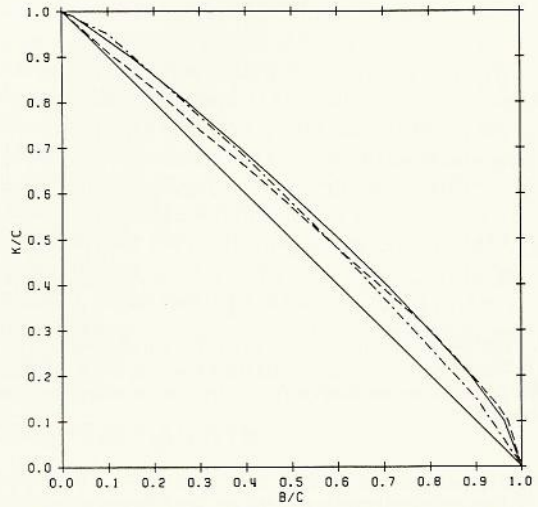


Fig. 6. Asymptotic diffuse attenuation coefficient dependence on $b$ and $c$. The upper solid curve is the result of Prieur and Morel, and the lower solid curve is the prediction of the SA approximation. The dashed–dotted curve is the SAA prediction, and the dashed curve is a two-stream approximation.

where $g$ is a dimensionless quantity. In fact, $K_d(\infty)$ is the solution of the eigenvalue problem

$$N(\mathbf{n}) = \frac{b/c}{1 - \eta(n)K_d(\infty)/c} \int d^2n' P(\mathbf{n}, \mathbf{n}')N(\mathbf{n}'). \tag{13}$$

Prieur and Morel[9] numerically solved this eigenvalue problem for several types of phase function. The result obtained using a phase function representing ocean water is the upper solid curve in Fig. 6. The lower solid curve is a straight line and is the solution predicted by the SA solution. The SAA expression is

$$\frac{K_d(\infty)}{c} = 1 - \frac{b}{c} + \left[\mu \frac{b}{c}\left(1 - \frac{b}{c}\right)\right]^{1/2}$$

or

$$K_d(\infty) = a + 1/l. \tag{14}$$

This form for $K_d(\infty)$ reinforces the interpretation of $l$ as a diffusion length. The dashed–dotted curve in Fig. 6 is this expression for $K_d(\infty)/c$ with the choice $\mu = 0.026$. The SAA solution agrees with the numerical solution best in the weak-scattering region $b/c < 1/2$.

Equation (13) is an equation for the eigenvalue $K_d(\infty)/c$ and the eigenvector $N(\mathbf{n})$. By using a multistream approximation, an explicit expression for $K_d(\infty)/c$ as the minimum eigenvalue of a particular matrix can be constructed. In this approach, the radiant energy contributed by the Sun to the underwater distribution is described by the distribution $L^0(\mathbf{n})$ at the surface. The RT problem to solve is

$$\left(\cos\theta \frac{\partial}{\partial z} + c\right) L(z, \mathbf{n}) = b \int d^2n' P(\mathbf{n}, \mathbf{n}')L(z, \mathbf{n}'),$$

$$L(z = 0, \mathbf{n}) = L^0(\mathbf{n}).$$

The multistream prescription for the $M$ directions $\mathbf{n}_k$ ($k = 1, \ldots, M$) is to make the replacements

$$L(z, \mathbf{n}) \to L_k(z) = [\mathbf{L}(z)]_k,$$

$$d^2n' P(\mathbf{n}, \mathbf{n}') \to P_{kk'} = (\mathcal{P})_{kk'}.$$

The RT equation is replaced by the collection of $M$ equations

$$\left\{n \frac{\partial}{\partial z} + c\right\} \cdot \mathbf{L}(z) = b\mathcal{P} \cdot \mathbf{L}(z) \tag{15}$$

and the initial conditions

$$\mathbf{L}(z = 0) = \mathbf{L}^0,$$

where

$$(n)_{kk'} = \delta_{kk'} \cos\theta_k.$$

Suppose that the matrix $\mathcal{M} = n^{-1} \cdot (c - b\mathcal{P})$ has the eigenvalues and eigenvectors $m_\alpha$ and $\psi_\alpha$, respectively. A rearrangement of terms in Eq. (15) leads to

$$\left\{\frac{\partial}{\partial z} + m_\alpha\right\} L_\alpha(z) = 0$$

and has the solution

$$\mathbf{L}(z) = \sum_\alpha \psi_\alpha L_\alpha{}^0 \exp(-m_\alpha z),$$

where

$$L_\alpha{}^0 = \psi_\alpha \cdot \mathbf{L}^0.$$

At any depth, the diffuse attenuation coefficient is

$$K_d(z) = \frac{\sum_\alpha m_\alpha \Omega_\alpha L_\alpha \exp(-m_\alpha z)}{\sum_\alpha \Omega_\alpha L_\alpha \exp(-m_\alpha z)},$$

where

$$\Omega_\alpha = \sum_k \Delta\Omega_k (\psi_\alpha)_k$$

and $\Delta\Omega_k$ is the solid angle of the $k$th stream. At asymptotic depths the only term to survive in each sum over $\alpha$ is the one corresponding to the minimum positive indefinite eigenvalue $m_\alpha$. Negative eigenvalues of $\mathcal{M}$ exist in general but are not included in the solution since they correspond to RT in the $-\hat{z}$ direction out of the ocean surface. The multistream approximation to the asymptotic diffuse attenuation coefficient is

$$K_d(\infty)/c = \lambda_{\min},$$

where $\lambda_{\min}$ is the minimum positive indefinite eigenvalue of the matrix

$$\lambda = n^{-1} \cdot \left(1 - \frac{b}{c}\mathcal{P}\right).$$

This is a general solution using only a multistream approximation and should converge to the exact asymptotic diffuse attenuation coefficient in the large-$M$ limit.

As an example of the predictions of this minimum eigenvalue formulation, a two-stream approximation can be

solved analytically and is the simplest case possible. The $k = 1$ stream corresponds to the forward-scatter direction, and $k = 2$ is the backward direction. For $M$ streams, the normalization of the phase function implies that

$$\sum_{k'} P_{kk'} = 1.$$

The simplest phase matrix is also symmetric:

$$\mathcal{P} = \begin{bmatrix} P & 1-P \\ 1-P & P \end{bmatrix}.$$

The $\lambda$ matrix has one positive and one negative eigenvalue. The minimum (and only) positive indefinite eigenvalue is

$$\left.\frac{K_d(\infty)}{c}\right|_{2\text{-stream}} = \lambda_{\min}$$

$$= \left[\left(1 - \frac{b}{c}P\right)^2 - \left(\frac{b}{c}\right)^2 (1-P)^2\right]^{1/2}. \quad (16)$$

The dashed curve in Fig. 6 is Eq. (16) with the choice $P = 0.85$. In the scatter-dominated limit $b/c > 1/2$, Eq. (16) can be made to agree reasonably with the numerical result. Presumably the choice of a larger $M$ would lead to better agreement.

A similar result for the two-stream approximation was obtained by Aas,[16] using a detailed analysis of the coupled differential equations for the upward and downward irradiance.

Before the radiance distribution reaches the asymptotic state with a constant diffuse attenuation, $K_d$ depends on both depth and the position of the Sun in the sky. However, the SA solution fails to predict any dependence on solar position:

$$K_d^{\mathrm{SA}}(z) = a + \frac{2}{z},$$

whereas the SAA solution does have at least a simple dependence:

$$K_d^{\mathrm{SAA}}(z) = a + \frac{\tanh(x)}{l} + \frac{\sin^2(\theta_{\mathrm{Sun}})}{2b\mu l^2} Q(x),$$

where $x = z/l$ and

$$Q(x) = 8\frac{\coth(2x)}{\sinh(2x)} - \frac{1}{\sinh^2(x)}.$$

To evaluate the degree of improvement in the SAA solution over the SA solution, Fig. 7 shows the $K_d(z)$ predicted by these two solutions and data points obtained by Helliwell and Gasster from a finite-difference code that solves the RT equation in one spatial dimension[10] in a way similar to the $S_n$ method of Carlson. The scheme is described in detail in Ref. 11. The choice of parameters is

$$a = 0.12\ \mathrm{m}^{-1},$$

$$b = 0.28\ \mathrm{m}^{-1},$$

$$\theta_{\mathrm{Sun}} = 27°,$$

$$\mu = 0.035$$

and corresponds to the Lake Pend Oreille conditions. Neither of the approximate solutions is adequate at shallow depths, although the SAA solution remains within 5% of the numerical result as the depth becomes large.

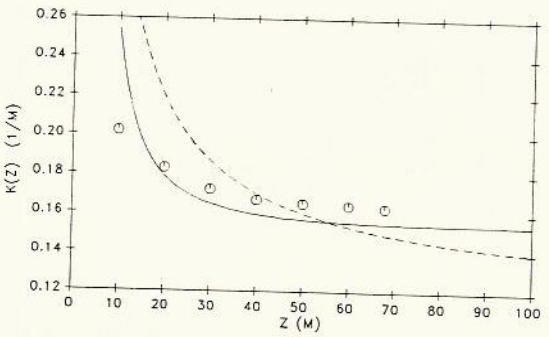


Fig. 7. Diffuse attenuation $K_d(z)$ as a function of depth. The solid curve is the SAA prediction, the dashed curve is the SA prediction, and the data points are from a finite-difference solution of the RT equation.

## 6. CONCLUSIONS AND DISCUSSION

As outlined in Sections 2 and 3, the two small-angle approximate solutions have a common origin and indeed differ in their path-integral expressions by only one term. The motivation for including the extra term follows from a standard Laplace method argument for integral approximation[17]: The leading-order approximation must include all terms through quadratic in the exponent of the integrand in order to ensure proper location of the peak of the integrand and approximation of its width. Despite this slight difference in the initial stage of approximation, the comparisons in Sections 4 and 5 show that the two approximate solutions are qualitatively different and that the SAA solution is more successful than the SA solution in exhibiting behaviors that are consistent with experimental and numerical data. The difference is characterized by a diffusion length $l$, which limits the distance through which radiative transfer can be regarded as a diffusive random walk. The inclusion of still higher-order terms may again change and improve the resulting predictions by substantial amounts. A calculation of the next few terms in the approximation of the integrand could help in estimating how many terms are needed in total to improve the large-angle behavior of the solution.

From Figs. 3 and 4, the introduction of a diffusion length allows the SAA solution for the solar peak to attenuate with depth at essentially the same rate as the measured distribution peak. However, the small-angle approximation still breaks down within 10°–15° of the peak. Higher-order corrections to the SAA approximation must contribute up to several orders of magnitude to the distribution at larger angles.

The comparison between approximate solutions and experimental data for the solar width (Section 4) was accomplished by using measured properties of the radiance distribution at a large (asymptotic?) depth to estimate the optical parameters $a$ and $\mu b$. Since the phase function for ocean water is nearly independent of location and of the magnitude of the scattering coefficient $b$, an estimate of $\mu = 0.03$ could be reasonable. Indeed, with this choice, the values $b/c = 0.5$ and $K_d/c = 0.57$ are obtained, which is consistent with the

numerical results in Fig. 6. The agreement suggests that simultaneous measurements of the width of the solar distribution and the diffuse attenuation coefficient can be combined with Eqs. (12) and (14), and with the mean-square width of the phase function, to obtain estimates of $c$ and $b$ in the ocean. This scheme assumes that the ocean is homogeneous with depth, whereas it typically is stratified. A stratified ocean could be accommodated by a modified scheme, however, because the path-integral formulation and approximate evaluation can be constructed with stratified optical coefficients. The resulting scheme would require the combination of measurements from the surface to the maximum depth of interest.

## ACKNOWLEDGMENTS

I would like to thank Robert Kelly and Samuel Gasster for interesting discussions on optics and oceanography. I am grateful to William Helliwell for providing the numerical data on the diffuse attenuation coefficient. The preparation of this manuscript was supported in part by Areté Associates.

## REFERENCES

1. L. S. Dolin, "Solution of the radiative transfer equation in a small-angle approximation for a stratified turbid medium with photon path dispersion taken into account," Izv. Atm. Ocean. Phys. **16,** 34–39 (1980); W. H. Wells, "Theory of small angle scattering," AGARD Lecture Series No. 61 on Optics of the Sea (NATO, Paris, 1973; National Technical Information Service, Springfield, Va.), pp. 3.3-1–3.3-19; D. Arnush, "Underwater light-beam propagation in the small-angle scattering approximation," J. Opt. Soc. Am. **62,** 1109–1111 (1972).
2. L. B. Stotts, "Limitations of approximate Fourier techniques in solving radiative-transfer problems," J. Opt. Soc. Am. **69,** 1719–1723 (1979).
3. A. Ishimaru, *Wave Propagation and Scattering in Random Media* (Academic, New York, 1978), Vol. 2, Chap. 14.
4. G. N. Plass and G. W. Kattawar, "Monte Carlo calculations of radiative transfer in the Earth's atmosphere–ocean system: I. Flux in the atmosphere and ocean," J. Phys. Oceanogr. **2,** 139–145 (1972).
5. L. R. Thebaud and S. J. Gayer, "Calculation of lidar beam spread in stratified media," in *Ocean Optics VII*, M. A. Blizard, ed., Proc. Soc. Photo-Opt. Instrum. Eng. **489,** 236–247 (1984).
6. J. Tessendorf, "Radiative transfer as a sum over paths," Phys. Rev. A **35,** 872–878 (1987).
7. J. E. Tyler, "Radiance distribution as a function of depth in an underwater environment," Bull. Scripps Inst. Oceanogr. **7,** 363–411 (1960).
8. M. Browne and R. A. Axford, "Angular width of the downwelling solar radiance profile as a function of depth," in *Ocean Optics VIII*, M. A. Blizard, ed., Proc. Soc. Photo-Opt. Instrum. Eng. **637,** 91–94 (1986).
9. L. Prieur and A. Morel, "Etude theorique du regime asymptotique: relations entre caracteristiques optiques et coefficient d'extinction relatif a la penetration de la lumiere du jour," Cah. Oceanogr. **23,** 35–48 (1971).
10. W. S. Helliwell and S. D. Gasster, "Obtaining inherent water optical properties from apparent water optical properties," in *Ocean Optics IX*, M. A. Blizard, ed., Proc. Soc. Photo-Opt. Instrum. Eng. **925** (to be published).
11. W. S. Helliwell, "Finite-difference solution to the radiative transfer equation for in-water radiance," J. Opt. Soc. Am. A **2,** 1325–1330 (1985).
12. R. P. Feynman and A. R. Hibbs, *Quantum Mechanics and Path Integrals* (McGraw-Hill, New York, 1965).
13. R. W. Preisendorfer, *Radiative Transfer on Discrete Spaces* (Pergamon, New York, 1965), Chap. 11.
14. R. W. Preisendorfer, *Hydrological Optics*, PB-259 796 (National Technical Information Service, Springfield, Va., 1976), Vol. 1.
15. R. W. Preisendorfer, "Theoretical proof of the existence of characteristic diffuse light in natural waters," J. Mar. Res. **18,** 1–9 (1959).
16. E. Aas, "Two-stream irradiance model for deep waters," Appl. Opt. **26,** 2095–2101 (1987).
17. C. M. Bender and S. A. Orszag, *Advanced Mathematical Methods for Scientists and Engineers* (McGraw-Hill, New York, 1978), Chap. 6.